

BACKGROUND EFFECTS ON REFLECTANCE AND DERIVATIVES IN AN OPEN-CANOPY FOREST  
USING AIRBORNE IMAGING SPECTROMETER DATA

Yoshio Awaya\*, John R. Miller\*\* and James R. Freemantle\*\*

\*Forestry and Forest Products Research Institute, P.O.Box 16, Tsukuba, Ibaraki 305, JAPAN

\*\*Institute for Space and Terrestrial Science, 4850 Keele St., North York, Ontario, M3J 3K1 CANADA

Commission VII

ABSTRACT:

Though the relationship between tree biomass (as indicated by basal area, leaf area index, etc.) and reflectance or vegetation indices has been studied in depth, crown closure has generally received less attention. However, if the effects of forest background components (soils, snow etc.) on reflectance are not negligible, they should also be taken into account in data analyses. Though the forest floor background is generally not homogeneous and is very difficult to include in analyses, a fresh snow background makes it much easier. Compact Airborne Spectrographic Imager (CASI) data and aerial video data, which were acquired over an open-canopy forest on snow-covered ground in Santiam Pass, Oregon, were used to derive reflectance spectra and crown closure, respectively. The background contribution in the airborne spectra over a forest were studied with respect to the relationship between crown closure and reflectance. An exponential function was found to be representative of the relationship between reflectance and crown closure at each wavelength. Also, the effects due to the radiance difference between foreground and background reflectance on second derivative spectra of the CASI data and component mixture simulations based on the exponential function were examined with respect to crown closure. The comparison showed that the spectral radiance difference causes a curvilinear relationship between crown closure and the second derivative amplitude. Also, the non-linear background spectrum causes shifts in the peak positions in the second derivative as a function of crown closure variations.

KEY WORDS: Airborne Imaging Spectrometer, Forest Background, Crown Closure, Reflectance

1. INTRODUCTION

Vegetation biomass, including its elements (leaf area index (LAI), green phytomass, basal area, timber volume etc.) has been studied extensively with regard to its relationship with reflectance or vegetation indices using both airborne and spaceborne sensor data. The relation to crown closure, however, has received less attention. In a study by Ormsby et al. (1987) a linear relationship was reported with high correlation between the simple ratio and fractional vegetation within 125 by 125 pixels in Landsat MSS data. However, there are various types of vegetation and different soils in various proportions within a pixel, and the effects of background components are not readily quantified.

In sparse canopies the reflectance contribution of the background component is too large to be negligible, and the background effect should be taken into account in data analyses (e.g. relationship between biomass and reflectance). However, it has been pointed out that the influence of a background component such as soil which has a weak curvilinear spectral pattern can be removed by derivatives (Hobbs and Mooney, 1989; Demetriades-Shah et al., 1990). Derivative analysis has gained acceptance as an analytical tool in forest optical sensing, for example in vegetation vitality analysis (Boochs, et al. 1990), leaf chemistry analysis (Card et al. 1988) and analysis of forest canopy characteristics (Wessman et al. 1987). Airborne imaging spectrometers make it possible to acquire canopy level continuous spectra over forests from aircraft (Miller et al. 1987) and to apply derivatives to a forest characteristics analysis (Wessman et al. 1987; Rock et al. 1988).

The advantages of derivatives are widely recognized and their application will be increased. For instance, the applicability of the second derivative for the absorbed photosynthetically active radiation of forest canopy was pointed out by a simulation using the SAIL model (Hall et al. 1990). However the influence of background components has been poorly analyzed numerically.

Any spectral influence caused by a combination of background component spectra and canopy geometry are expected to exist within the spectra in open canopy forests, even in derivative spectra.

This paper aims at an analysis of background component effects on reflectance and derivative spectra as it relates to crown closure using Compact Airborne Spectrographic Imager (CASI) data from an open canopy forest. Also the implications of these results on the use of the second derivative to estimate APAR is examined.

2. MATERIALS AND METHODS

2.1 The Study Site

Santiam Pass (44°25'N, 121°51'E) is located in the mid-west of Oregon in the Cascade Mountains (Figures 1 and 2). The elevation of the study site is about 1450m above sea level and the topography is very flat. The forest is composed of several conifer species, subalpine fir (*Abies amabilis*), grand fir (*Abies grandis*), mountain hemlock (*Tsuga mertensiana*), lodgepole pine (*Pinus contorta*), Engelmann spruce (*Picea engelmannii*) and western white pine (*Pinus monticola*). The trees are quite homogeneous in height and are distributed in clumps.

CASI overflights of the study site took place on August 13, 1990 (The data used this study was obtained at around 11:34 AM local time.) and on May 21, 1991 (between 12:27 AM to 12:46 AM.). The solar azimuth and zenith angles were 164° and 30° in 1990 and 196° and 25° in 1991, respectively. The 1990 flight line was directed from the south-east to north-west covering forests and marshes. In 1991 one flight line was oriented from east to west covering the forest and the other oriented from the south to north covering a ground calibration target. Video imagery was obtained during the flight coinciding with CASI data acquisition.

The test site is spread along Highway 20, called Santiam Highway. The forest floor was evenly covered with fresh snow which had fallen a few days



Figure 1. Photograph of the study site taken on May 14, 1991.

before the 1991 flight.

## 2.2 Calibration Target Measurements

Field spectra were acquired for ground calibration targets under natural illumination using a Spectron Engineering SE-590 field spectrometer. The spectral resolution and spectral coverage of the spectrometer are 12 nm and from 380 to 1100 nm, respectively. The spectral measurements were done under a clear sky at about 4 PM on the same day of the 1991 CASI flight. A gravel pit near the test site was chosen as the calibration target and its spectral reflectance measured. Spectra were also obtained from snow and a Labsphere spectralon white standard reflectance panel. The spectrometer was positioned about 1 meter above the targets while viewing in the nadir direction. Both the gravel and snow spectra were converted into a reflectance by ratioing with the spectralon panel spectra (Figures 3 and 6A). These measured reflectances of the ground calibration targets were used to convert the CASI radiance data into reflectance, thereby removing atmospheric absorption features (Freemantle et al. 1992).

## 2.3 The Compact Airborne Spectrographic Imager

The Compact Airborne Spectrographic Imager (CASI) acquires data in both a spectral mode and a spatial mode in several flight lines. In this study, only the spectral mode data were analyzed.

The CASI data is digitized to 12 bits and provides

spectral coverage from 418 to 927 nm with 288 channels, at a nominal spectral resolution of 2.5 nm; the swath width of 35° can be sampled using up to 39 view directions (Anger et al. 1990). Each flight was at an altitude of 1800 m above ground level. The approximate pixel size for the CASI spectral mode data in this study was 2 X 9 m. The east to west flight data (EW CASI data) from 1991 was used for the crown closure study, and the south to north flight data (SN CASI data) from 1991 was used to acquire CASI radiance data from ground calibration targets. The 1990 flight data (1990's CASI data) was used to derive a vegetation-free wet soil spectrum.

A total of 3 spectral mode pixels from the SN CASI data were identified as dry pure gravel pixels located near the ground measurement location. No vegetation contamination or adjacency effect was identified in the spectrum of each pixel. The gravel reflectance from field measurements with Spectron SE-590 were applied to the CASI data radiance calibration to provide reflectance values. Each gravel pixel of the SN CASI data was tested and an average spectrum of two of them was used for the conversion to reflectance thereby producing somewhat noisy calibrated reflectance values. Cross calibration of reflectances between the 1990 CASI data and the 1991 CASI data was carried out using the asphalt pixels of Santiam Highway common to both 1991 and 1990 data.

## 2.4 Training Area Selection and Crown Closure Interpretation

The aerial video was digitized and converted into 35mm slides. The slides were projected on a dot matrix screen and the EW CASI data were displayed on a SUN-3 display, then the training areas were selected from the EW CASI data referring to the projected slides. As trees tended to form clumps, the training areas had to be carefully chosen from evenly populated tree areas. As the EW CASI data were acquired from a 35 degree swath angle, bi-directional reflectance features of the tree canopies (Asrar, 1989) can be expected to affect the observed radiance data due to the sun's azimuth angle to the flight direction and the wide swath angle. Consequently, the training areas were selected from the 9th to 23rd view directions (and mainly from the 10th to 18th columns) yielding data within ± 10 degrees of nadir thereby minimizing bi-directional reflectance variations and a marginal effect on the snow cover along the Santiam Highway.

The crown closure of each training area was measured in the following manner: 1) slides were projected on a 7 mm interval dot matrix sheet and the boundary of each pixel was carefully drawn on it. (Each pixel occupied 7 by 3 dots or 6 by 3 dots on the matrix sheet), 2) crown closures and snow cover were measured separately for each pixel, then disagreement between crown closure and snow cover measurements was examined, and 3) measurement was repeated until the disagreement became less than 2 dots for each pixel and the results were averaged for each training area. Thirty eight training areas were chosen.

Training pixels were selected from the EW CASI data simultaneously with the crown closure measurement, and saturated pixels were carefully checked according to the shape of each spectrum and discarded from each training area data. Then the crown closure of the training area was recalculated. The minimum number of pixels per training area was 5 and the CASI reflectance

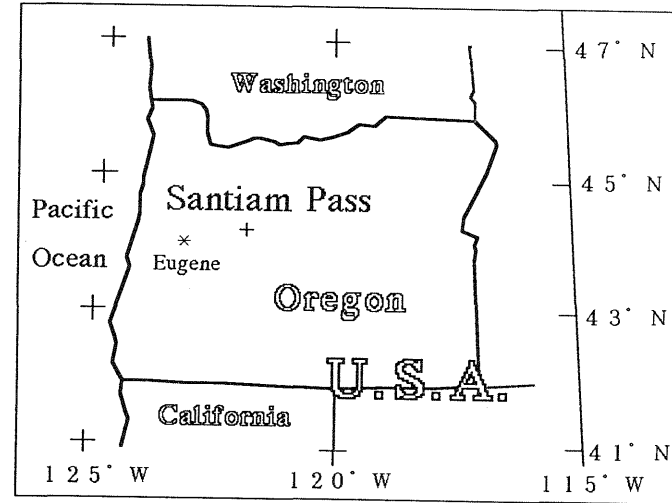
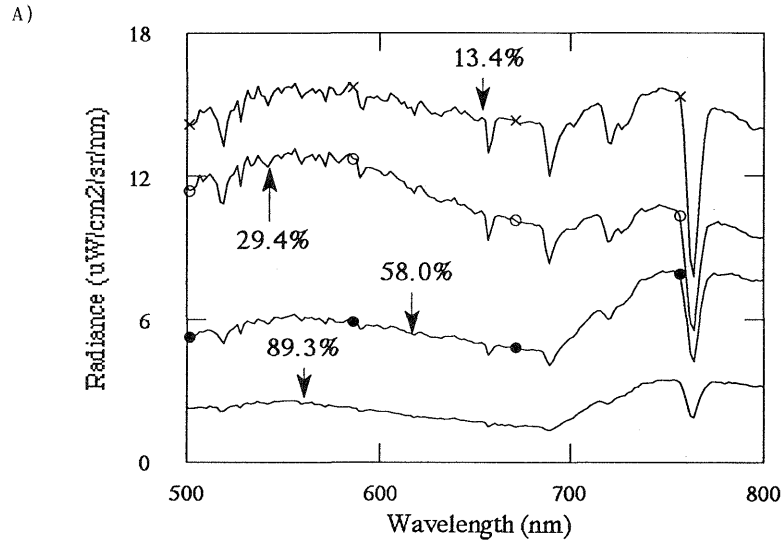


Figure 2. Location of the study site.

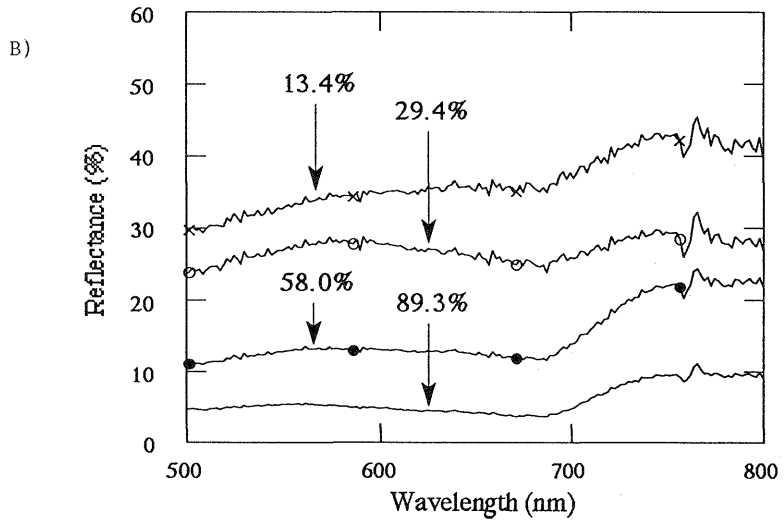


Figure 4. CASI radiance spectra 4A and their calibrated spectra 4B with different crown closures.

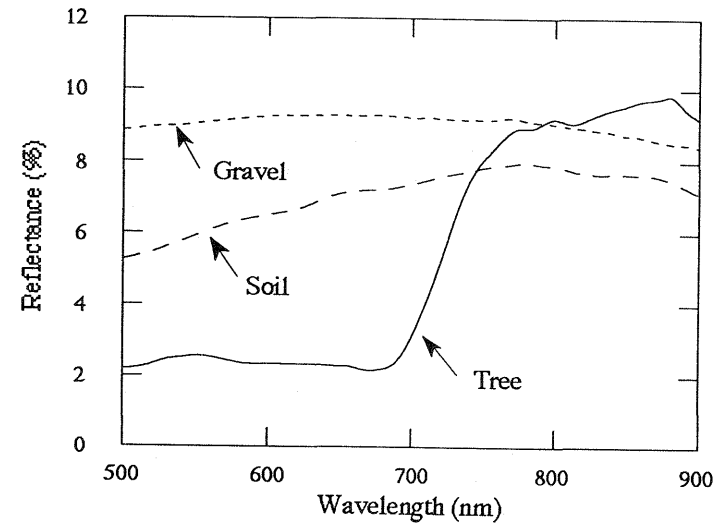


Figure 3. Field spectrum of the gravel acquired with the SE-590 spectrometer, and fully closed tree and vegetation free spectrum of CASI data for spectral simulation.

Table 1. Regression coefficients of equations predicting reflectance from tree crown closure for selected 9 channels. Sample size is 38. Regression equation:

$$\text{Reflectance} = a * \exp(b * \text{Closure})$$

Wavelength	a	b	r	r**2
500 nm	45.79	-0.024569	-0.959	0.919
550 nm	50.29	-0.02382	-0.959	0.920
600 nm	54.04	-0.024924	-0.962	0.926
650 nm	55.90	-0.026263	-0.962	0.925
680 nm	56.57	-0.026997	-0.960	0.921
700 nm	54.73	-0.023905	-0.958	0.917
750 nm	52.60	-0.016594	-0.934	0.873
780 nm	49.90	-0.015692	-0.927	0.859
800 nm	48.69	-0.014622	-0.928	0.861

spectra in each training area were averaged by each spectral channel.

### 3. ANALYSIS AND RESULTS

#### 3.1 Airborne Spectral Measurements

Some of the radiance and reflectance spectra acquired by CASI are shown in Figure 4. Strong spectral absorption in the visible region is clearly observed and relatively small spectral changes are clear in the near infrared region. The curves give a clear understanding of reflectance changes according to the different crown closures. However, as the reflectance becomes greater, the amplitude of spiky noise also becomes greater. The intensity of the noise is very great in the reflectance spectra of the small crown closure. This indicates that strong scattering occurs on the snow surface and disturbs clear observation of the spectra.

#### 3.2 Crown Closure and Reflectance

An exponential function was fitted to the inferred crown closure and the corresponding reflectance values for all the training data, averaged in intervals of 5 consecutive spectral channels over the entire spectral coverage of CASI, according to:

$$\text{Ref}(i) = a * \exp(b * \text{Crown}) \quad (1)$$

where

- a, b : constants
- Crown : Crown closure
- Ref(i): Reflectance at i-th channel averaged over 5 channels

Table 1 shows the results of regression between crown closure and reflectance for the exponential function at the 9 selected spectral channels. Coefficients of determination for the visible channels exceed 0.9 and exceed 0.85 in near infrared channels. Figure 5 presents scattergrams between the crown closure and reflectance of training areas for 680nm and 780nm as samples of the relationships in the visible (VIS) and near infrared (NIR) regions respectively. The curves at 680nm and 780nm are very similar. However since snow reflectance in VIS is higher than that in NIR, whereas tree reflectance in VIS is significantly smaller than that in NIR, the exponential curve slopes in NIR are gentler than those in VIS (Table 4). An exponential curve is seen to be representative of the reflectance variation with crown closure throughout the entire wavelength range of the CASI data. This implies that the snow-covered canopy floor has a similar effect over the entire spectral range. Similar curves have been observed using Landsat TM data for a forest

canopy on a snow covered surface (Leckie, 1991) and using Landsat TM simulator data for the LAI of coniferous forests (Peterson et al., 1987) in the red channel.

#### 3.3 Spectral Simulation

It is instructive to perform a simple simulation of the expected reflectance versus canopy closure relationships from the reflectance spectra of the primary scene components. For this purpose the reflectance spectra of a fully-closed forest canopy and vegetation-free wet soil were derived from the EW 1991 CASI data and the 1990 CASI data, respectively, and these spectra were smoothed to remove noise. Snow spectra were derived from the field measurements.

Forest reflectance spectra for different crown closures were then simulated by an exponential function pairing the closed forest and the snow spectra (tree-snow), or the closed forest and the soil spectra (tree-soil) as the spectrum of a completely closed forest (100% crown closure) and the spectrum of a completely open area (0% crown closure) respectively.

The simulated spectra (Figure 6A.) show the basic spectral features of the forest spectra extracted from the CASI data (Figure 4B) but with a tendency to overestimate the reflectance in the visible region at small crown closures.

#### 3.4 Derivative spectral analysis

In order to examine the potential of derivative spectral to discriminate against variations in background amount the CASI reflectance spectra were first smoothed to reduce noise using a linear-weighting running-average technique over 19 spectral channels according to:

$$\text{Refs}(i) = \sum_{j=-n,n} w(j) * \text{Ref}(i+j) \quad (2)$$

where

- w(j) : Linear weight for the (i+j)th channel for j = -n, -(n-1), ..., -1, 0, 1, ..., n
- w(j) = 1\*c, 2\*c, ..., n\*c, (n+1)\*c
- $\sum w(i+j) = 1$
- n : 2\*n+1 is the number of channels used for smoothing
- Ref(i+j): Reflectance of the (i+j)th channel
- Refs(i) : Smoothed reflectance of the i-th channel

Reflectance values from two channels with an interval of one channel were differenced to yield the first derivative according to:

$$\text{Ref}'(i) = (\text{Ref}(i+1) - \text{Ref}(i-1)) \quad (3)$$

where

- Ref(i+1): reflectance of (i+1)th channel
- Ref'(i) : 1st derivative of i-th channel

This operation was applied for every channel except for the beginning and end channels. Similarly, using linearly weighted averages with 11 spectral channels on first derivative spectra followed by differencing as above the second derivative spectra were calculated.

The second derivative spectra of the CASI data (Figure 7) shows the same basic spectral pattern reported in analysis of ground spectral measurements (Demetriades-Shah, 1990) and in simulations by Hall et al. (1990). The two major peaks which appeared on both sides of the red edge

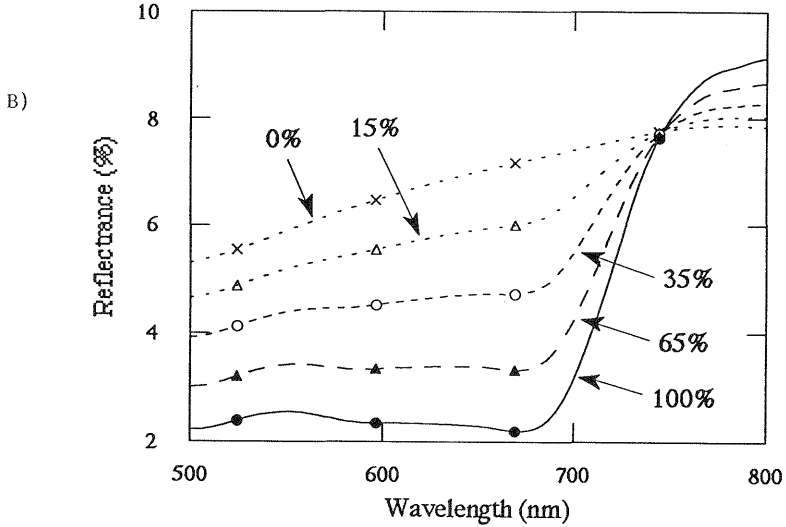
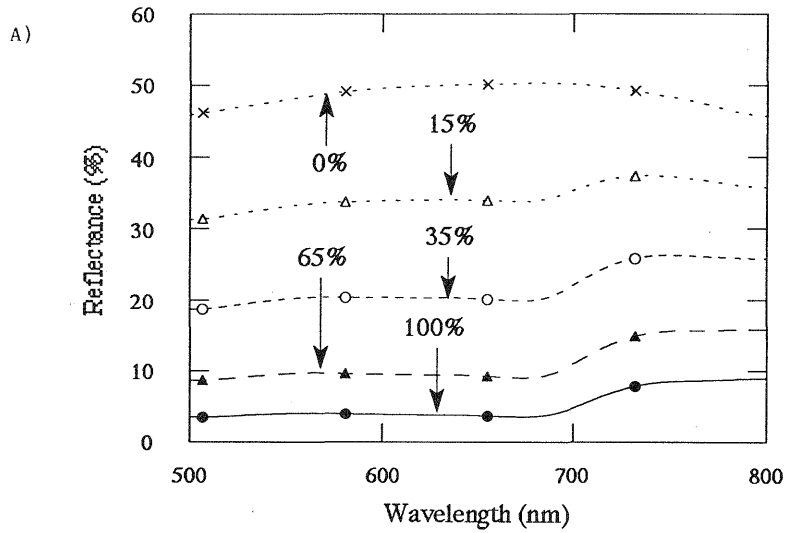


Figure 6. Simulated spectra by an exponential function using a fully covered forest spectrum as 100% crown closure and a snow spectrum as 0% crown closure 6A, and using the forest spectrum and a soil spectrum 6B.

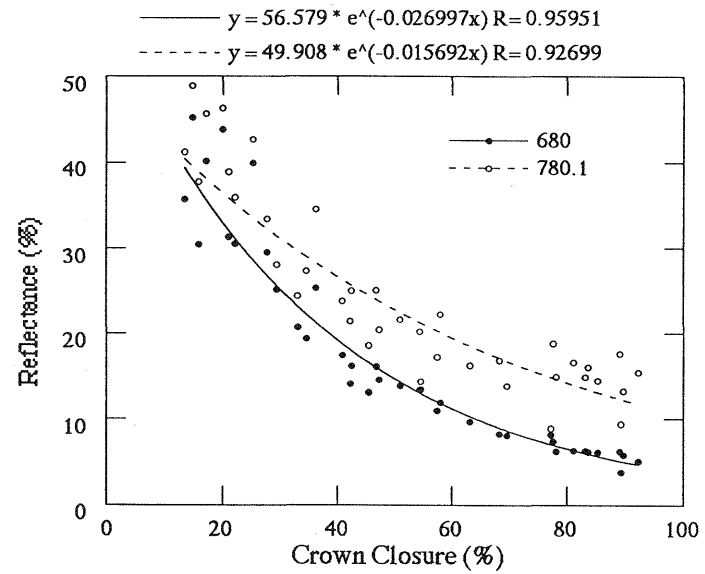


Figure 5. Scattergram of CASI reflectance vs. tree crown closure at 680nm (red well, visible) and 780nm. Reflectance was averaged over five channels covering about 9nm.

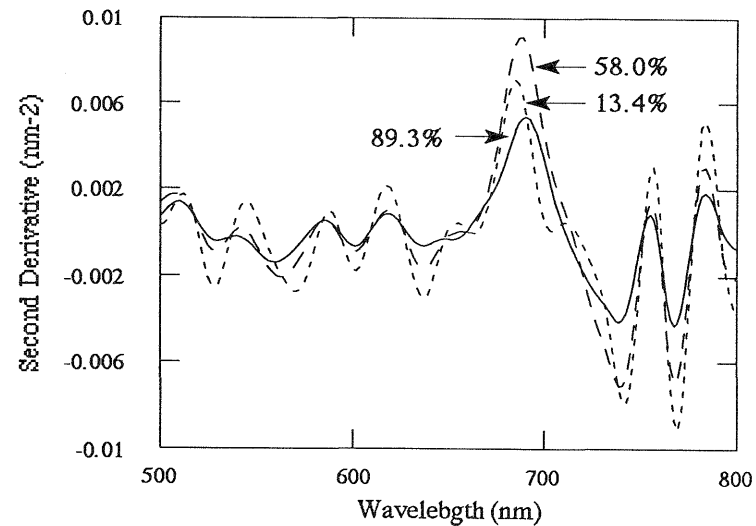


Figure 7. Second derivative spectra derived from CASI data.

at about 680 nm and 740 nm are those characteristic of vegetation spectra and are assigned special significance by Hall et al. (1990) in their simulation of relationships between second derivative spectra at 690 nm and 740 nm and APAR. However the observed second derivative spectra, especially for low crown closure sites, are uneven with small peaks throughout the entire spectral range and have additional prominent narrow peaks in NIR beyond 750 nm.

Derivatives of the our simulation spectra (both tree-snow and tree-soil combinations) were obtained in the same manner as for the derivatives of the CASI data. Eleven and seven channel weighted averages were used for the first derivative and the second derivatives, respectively. The large clear wave pattern was removed in the second derivative spectra of the two simulations (tree-snow and tree-soil simulations (Figures 8A and 8B). Clear major peaks appeared the same as in the CASI derivative. However the peak spectral position differs slightly between the tree-snow and tree-soil simulations.

#### 4. DISCUSSION

The exponential function was found to provide an excellent representation of the relationship between crown closure and reflectance of the open canopy forest in the visible and near infrared channels. As the tree height in the study area was quite homogeneous, the leaf area index of each tree was also presumed to be quite homogeneous. If the leaf area index were to vary significantly between trees corresponding variations would be expected in the near infrared reflectance reducing the curve fit correlation coefficients for the near infrared channels relative to the visible channels. As transmittance and reflectance are dominant in the near infrared wavelengths and absorption is dominant in visible wavelengths (Swain and Davis, 1978), the leaf area can be expected to affect the spectral response in a different manner at near infrared wavelengths compared to visible wavelengths. However the crown closure/reflectance curves for both the spectral channels do not differ greatly with a decreasing curvature in the near infrared channels. This supports homogeneity of leaf area per tree crown in each training area.

Sellers (1987) illustrated the dependence of canopy irradiance reflectance on canopy parameters LAI, leaf scattering coefficient and soil reflectance in both the visible and the near infrared regions using a two-stream model. The curves relating LAI and surface reflectance in his study are very similar to the curves in Figure 5. It is difficult to identify the key factor, crown closure or LAI, which controls the variation of canopy reflectance in this study. We have assumed that crown closure is well correlated with LAI in the training areas of this study.

Since the training areas provide a good spread of data making the curve at each channel (Figure 5), various kinds of functions (polynomials, exponential function, etc.) could probably yield excellent fits to the data. However it would not be easy to select which functional form is optimal for the regression. Vales and Bunnell (1988) reported that the exponential curve is the best form of regression for mean crown completeness and radiation through tree crowns as measured on the ground. This and Seller's simulation probably supports the application of the exponential function to the curve fitting. However as the reflectance at 100% crown closure, namely an

asymptotic value of the exponential function, is not 0, a modified exponential function ( $Y=K+a*\exp(b*X)$ ) may also be viewed favorably.

If the vitality of each tree in a forest is virtually constant, LAI will be closely related to APAR. The interpreted crown closure and the reflectance-crown closure curve supports this concept, and therefore the crown closure and reflectance relationship could be substituted for the APAR and reflectance relationship. Consequently, if the second derivative intensities of the CASI data show a clear relationship with crown closures, this would support the possibility of estimation of APAR by the second derivative (Hall et al. 1990) from airborne data.

A correlation plot (Figure 9) for the crown closure with the second derivative intensities of the CASI and simulated spectra reveals that a high correlation between the crown closure and the CASI second derivative intensities occur at wavelengths not expected from the simulation results. This is a result of noise on the computation of derivative spectra emphasizing the care required in interpretation of derivative analysis using noisy data.

The second derivative spectra of the CASI data were compared at several channels with the second derivative spectra of the tree-snow simulation. As the reflectance increased significantly at the red edge, the second derivative showed wide variation at the red well (680 nm) and the red edge shoulder (740 nm). Therefore good agreement with the second derivatives and the crown closure was expected at both channels. However, the second derivative spectra from the tree-snow and tree-soil simulation show more realistic patterns than the second derivatives of the CASI data. In general good agreement was not found between the CASI derivative intensities and the derivative intensities from the simulation. The relatively good agreement of the two derivative intensities found at 692.5 nm (Figure 10) is seen to break down as the crown closure exceeds 60%; a detailed analysis is necessary to understand the reason for this. A further investigation is also necessary to confirm any possibility of derivative application for the APAR analysis.

As the derivatives are sensitive to high frequency spectrum noise (Demetriades-Shah et al. 1990), the spiky noise in the CASI reflectance spectra disturbed the derivative analysis. Though the linear weighting average was very noise invariant compared with the ordinary average, the spiky noise was not removed sufficiently. Third and fifth order polynomials using 9 to 25 channels were also tested for smoothing, however, these results were poor. Some filtering, using for example a median filter, is necessary to remove noise. Fitting a single spectral curve around the red edge region is probably another possible choice for smoothing out noisy spectra (Miller et al., 1990). As reflectance spectra of snow free CASI data are usually smooth enough for derivatives of at least of the second order, the noisy data set in this study is probably a very special case.

The second derivative spectra of the tree-soil simulation were compared to the derivative spectra of the tree-snow simulation (Figure 8, 10). The following two tendencies were found. 1) spectral positions of peaks in the derivative spectra are shifted according to the relative differences in reflectances between the tree and the background object. However, selecting the maximum of the

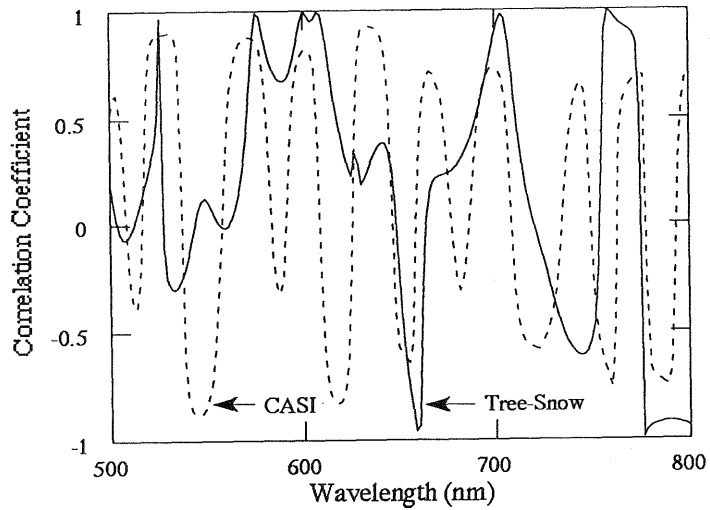


Figure 9. Correlation plot for crown closure and second derivative intensities of CASI spectra, tree-snow and tree-soil intensities.

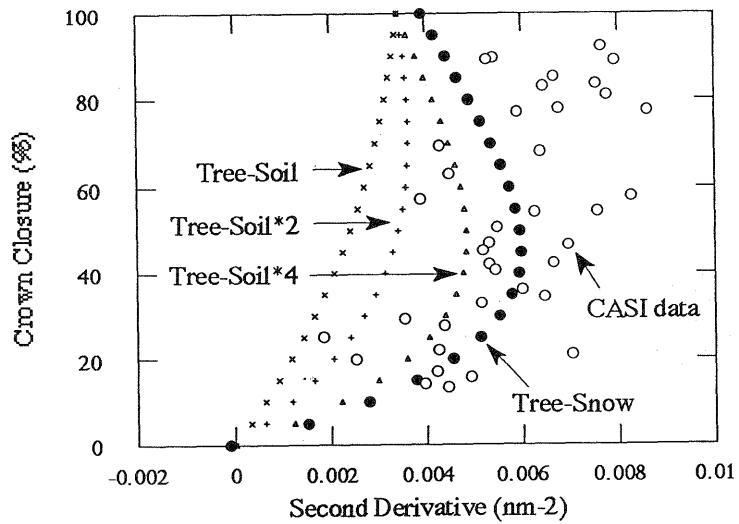


Figure 10. Second derivative intensities vs. crown closure at 690nm for CASI data and, tree-snow, tree-soil, tree-soil\*2 and tree-soil\*4 (the soil spectrum was multiplied by 2 and 4 respectively) simulation.

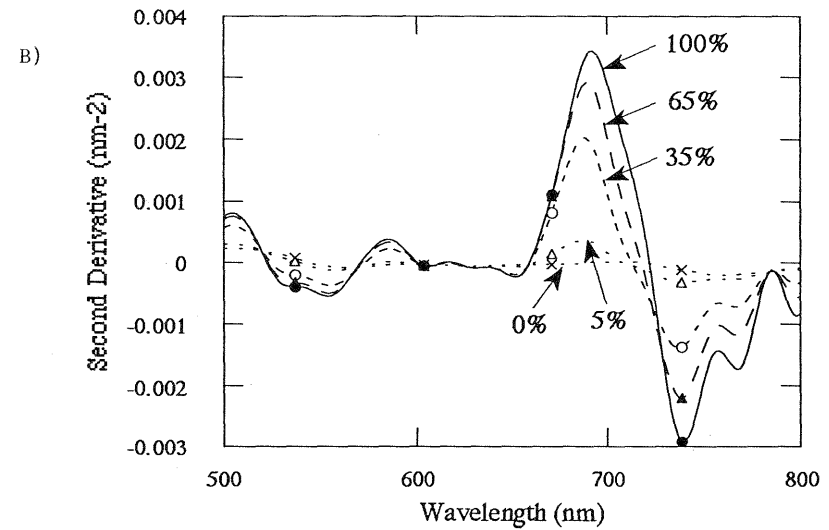
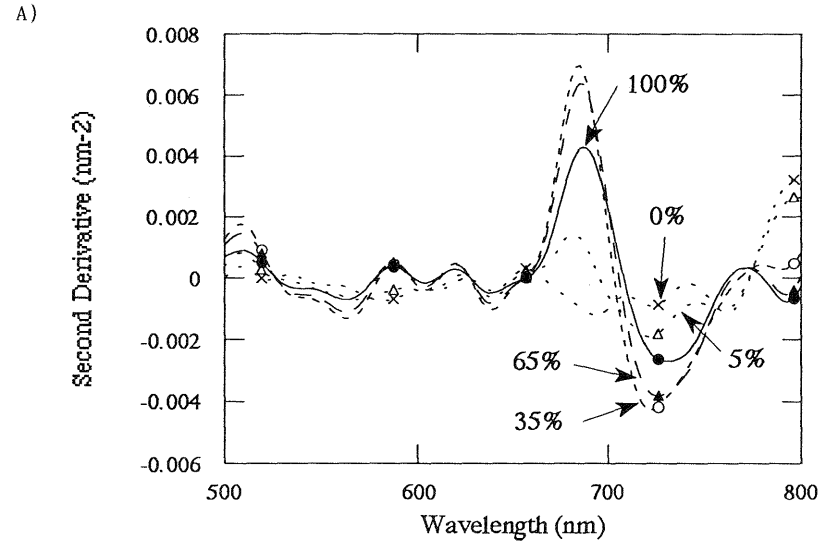


Figure 8. Second derivative spectra derived from the simulated spectra. Tree-snow 8A and tree-soil 8B.

derivative amplitude in the vicinity of a peak, 690nm for example, would give intensities which are relatively less affected by the background spectrum than with selecting at a specific wavelength 2) if the background reflectance is greater than the tree reflectance, a much greater curvature tendency appears in relating second derivative intensities to crown closure.

#### 5. CONCLUSION

The relationship between crown closure, as determined from aerial video images, and reflectance spectra, as determined from airborne digital imagery using the Compact Airborne Spectrographic Imager (CASI), has been found to exhibit an exponential behavior for each spectral channel. In addition, variations in CASI derivative spectra were examined as an alternate means of describing crown closure. The following additional results have emerged from the analysis of airborne spectra and component mixture simulations:

- 1) Increases in the reflectance difference between foreground (tree) and background (snow/soil etc.) resulted in increases in the curvature in the relationship between crown closure and the 2nd derivative amplitudes, and
- 2) non-linearity in the background reflectance spectra produced observable spectral shifts in the 2nd derivative curve peak, especially in the red edge of the vegetation spectra.

#### 6. ACKNOWLEDGMENTS

This study was executed using data acquired as part of our contribution to the 'Oregon Transect Ecosystem Research' project. The authors are grateful to project leaders Dr. David Peterson and Dr. Richard Waring for cooperation and support that made our participation in this study possible. The authors also appreciate the support of our colleagues, Peng Gong, Ruiliang Pu and Michael Belanger who carried out ground measurements with us.

#### 7. REFERENCES

- Anger, C. D., Babey, S.K. and Adamson, R. J. 1990. A new approach to imaging spectrometry. SPIE vol. 1298, pp 72 - 86.
- Asrar, G., 1989. Theory and Applications of Optical Remote Sensing. John Wiley and Sons, New York, pp.14-65.
- Boochs, F., Kupfer, G., Dockter, K. and Kupfer, G. 1990. Shape of the red edge as vitality indicator for plants. International Journal of Remote Sensing, 11-10:1741-1753.
- Card, D.H., Peterson, D.L., Matson, P.A. and Aber, J.D. 1988. Prediction of leaf chemistry by the use of visible and near infrared reflectance spectroscopy, Remote Sensing of Environment, 26:123-147.
- Demetriades-Shah, T.H., Steven, M.D. and Clark, J.A., 1990. High resolution derivative spectra in remote sensing. Remote Sensing of Environment, 33:55-64.
- Freemantle, J.R., Pu, R. and Miller, J.R. 1992. Calibration of imaging spectrometer data to reflectance using psuedo-invariant features, Proceedings of the 15th Canadian Symposium on Remote Sensing, June 2-4, 1992.
- Hall, F.G., Huemmrich, K.F. and Goward, S.N., 1990. Use of narrow-band spectra to estimate the fraction of absorbed photosynthetically active radiation. Remote Sensing of Environment, 32-1:47-54.
- Hobbs, R.J. and Mooney, H.A.(editors), 1989. Remote Sensing of Biosphere Functioning. Springer-Verlag, New York, pp.135-156.
- Leckie, D.G., 1991. Personal communication, Petawawa National Forestry Institute, Ontario, Canada.
- Miller, J.R., Hare, E.W., Hollinger, A.B. and Sturgeon, D.R., 1987. Imaging spectrometry as a tool for botanical mapping. In: Proceedings of SPIE-The International Society for Optical Engineering, San Diego CA, vol-834, pp.108-113.
- Miller, J.R., Hare, E.W. and Wu, J., 1990. Quantitative characterization of the vegetation red edge reflectance 1.An inverted-gaussian reflectance model. International Journal of Remote Sensing, 11:1755 - 1773.
- Ormsby, J.P., Choudhury, B.J. and Owe, M. 1987. Vegetation spatial variability and its effect on vegetation indices, International Journal of Remote Sensing, 8-9:1301-1306.
- Peterson, D.L., Spanner M.A., Running S.W. and Teuber K.B. 1987. Relationship of Thematic Mapper simulator data to leaf area index of temperate coniferous forests, Remote Sensing of Environment, 22:323-341.
- Rock, B.N., Hoshizaki, T. and Miller, J.R., 1988. Comparison of in situ and airborne spectral measurements of the blue shift associated with forest decline. Remote Sensing of Environment, 24:109-127.
- Sellers, P.J., 1987. Canopy reflectance, photosynthesis, and transpiration. II. The role of biophysics in the linearity of their interdependence. Remote Sensing of Environment, 21:143-183.
- Swain, P.H. and Davis, S.M.(editors), 1978. Remote Sensing: The Quantitative Approach. McGraw-Hill, New York, pp.231-241.
- Vales, D.J. and Bunnell, F.L., 1988. Relationships between transmission of solar radiation and coniferous forest stand characteristics. Agriculture and Forest Meteorology, 43:201-223.
- Wessman, C.A., Aber, J.D. and Peterson, D.L., 1987. Estimation of forest canopy characteristics and nitrogen cycling using imaging spectrometry. In: Proceedings of SPIE-The International Society for Optical Engineering, San Diego CA, vol-834, pp.114-118.